Experimental Evidence for Improved Confinement with Quasisymmetry in HSX

S. P. Gerhardt 1), A. Abdou 1), A. Almagri 1), D.T. Anderson 1), F.S.B. Anderson 1), D. Brower 2), J. Canik 1), C. Deng 2), W. Guttenfelder 1), K. Likin 1), S. Oh 1), J. Tabora 1), V. Sakaguchi 1), J. Schmitt 1), J.N. Talmadge 1), and K. Zhai 1)

1) The HSX Plasma Laboratory, University of Wisconsin-Madison
2) Electrical Engineering Department, University of California, Los Angeles

E-mail address of main author: spgerhar@students.wisc.edu

Abstract: Plasmas produced by second harmonic electron cyclotron heating (ECH) in the HSX stellarator provide the first evidence of transport improvement due to quasisymmetry in a stellarator. Comparisons are made between plasmas in the base quasihelically symmetric (QHS) configuration and two neoclassically degraded configurations which lack quasisymmetry (Mirror configurations). It is found that the plasma breakdown occurs more easily in the QHS configuration, indicating improved confinement of the breakdown electrons. The stored energy in the QHS configuration is up to six times larger than discharges in the Mirror configurations, and evidence is shown for enhanced prompt loss of trapped particles when the Mirror field is applied. The momentum damping rate is measured to be factors of three to four less in the QHS configuration than the Mirror configuration.

1. Introduction

Lack of symmetry in conventional stellarators leads to direct loss of trapped particles, enhanced neoclassical transport, and large parallel viscous damping of flows in all directions on a flux surface. The Helically Symmetric eXperiment (HSX) [1] solves this problem by introducing a direction of symmetry to the current free stellarator configuration: the strength of the magnetic field on a flux surface can be expressed in Boozer coordinates as $B/B_o=1+\varepsilon_H\cos(4\varphi-\theta)$, with φ the toroidal angle and θ the poloidal angle [2]. This restoration of symmetry improves particle orbits, drastically reduces the neoclassical transport, and introduces a direction of minimum flow damping. The quasisymmetry in HSX can be degraded by the introduction of an additional spectral component with toroidal mode number n=4 and poloidal mode number m=0, with minimal changes in the well depth, plasma volume, or rotational transform profile. When this extra field has its maximum at the location of the electron cyclotron heating (ECH) launching mirror, it is called the Mirror configuration. The configuration with the phase of this auxiliary field rotated toroidally by 45°, leading to a very deep minimum in the magnetic field at the ECH launching mirror, is called the antiMirror configuration. This paper presents the first experimental results demonstrating higher stored energy and better trapped particle confinement in the QHS configuration compared to the antiMirror configuration, and reduced viscous damping of flows in the QHS configuration compared to the Mirror case.

2. Studies of the Plasma Breakdown time in the Different Configurations.

The first test of quasisymmetry in HSX was done by determining how the breakdown time of the ECH plasma varied as a function of resonance location and machine configuration. The machine was filled with a constant bleed of hydrogen and the time between the start of the ECH pulse and the measurement of a small density (2×10^{10} cm^{-3}) was studied in different

configurations. Fig. 1 shows the results as a function of the location of the ECH resonance layer, for the QHS and antiMirror configurations. A normalized radius less than zero corresponds to heating on the inboard side of the torus. For both configurations, the minima of the breakdown times are centered on the magnetic axis to within experimental uncertainty. More importantly, the antiMirror configuration has a uniformly longer breakdown time.

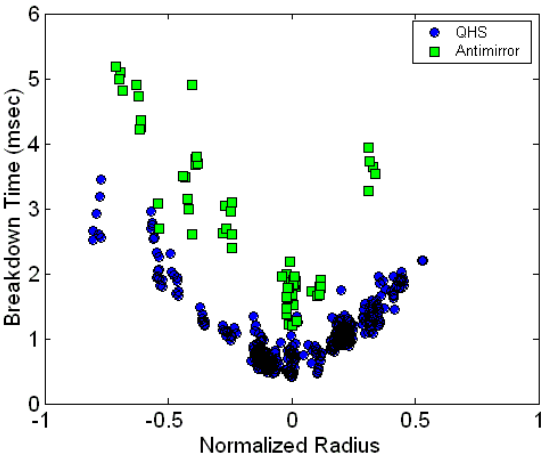

FIG. 1. Variation of the breakdown time with resonace location in the QHS and antiMirror configurations.

The breakdown time is connected to the confinement of the initial seed electrons [3]. To study their confinement, we have computed the collisionless orbits in Boozer coordinates of deeply trapped electrons in both the QHS and antiMirror configurations; the particles are launched on the low field side of the torus with an energy of 20 keV and pitch angle of 80°. The QHS orbit is shown in Fig. 2a, where it is apparent that the particle is executing a banana orbit in the helical well of the main n=4, m=1 component of the magnetic field spectrum, but never deviates substantially from its launch surface. In the antiMirror configuration shown in Fig. 2b, the particle is on a direct loss orbit and leaves the confinement volume.

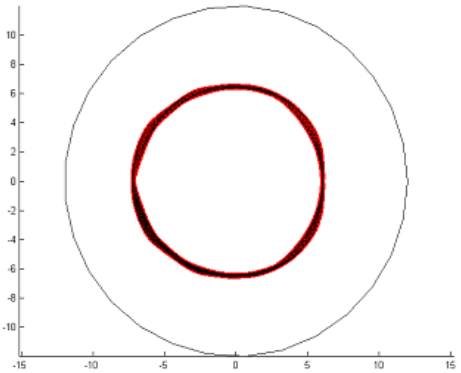

FIG. 2b. Orbit of a deeply trapped electron in the QHS configuration

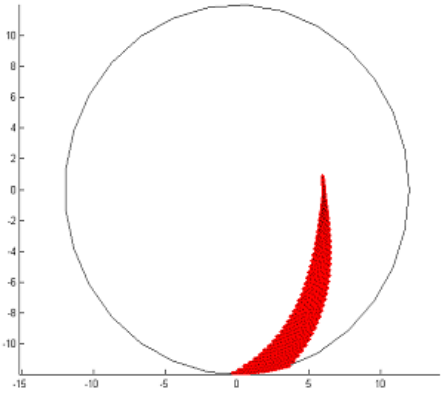

FIG. 2b. Orbit of a deeply trapped electron in the antiMirror configuration

3. Plasma Stored Energy and Direct Loss Orbits

The general characteristics of low density discharges in the QHS and

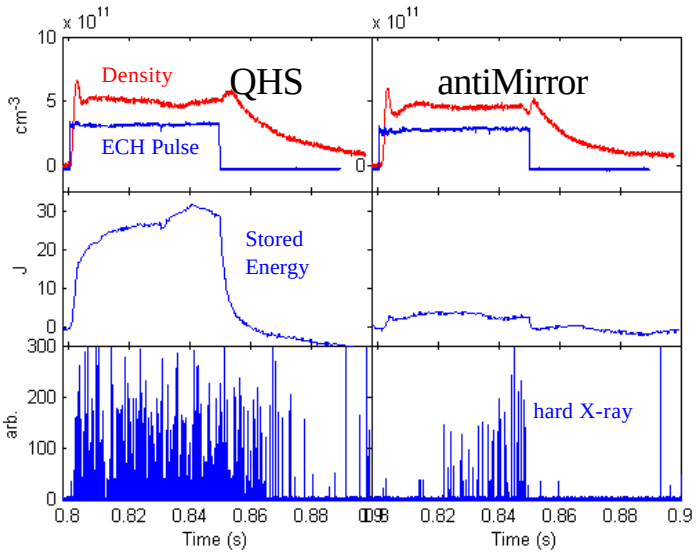

FIG. 3. Density, Stored Energy, and hard X-ray signals from similar QHS (left) and antiMirror (Right) discharges.

antiMirror configuration are shown in Fig. 3. Both discharges have an equilibrium density of $5x10^{11}$ cm^{-3}, but the stored energy of 30J in the QHS configuration is approximately six times larger than in the antiMirror configuration. Also shown are the pulses from a CdZnTe hard X-ray detector, located outside the vessel and sensitive to photons of energy greater than 25 keV. The hard X-ray flux is substantially higher in the QHS configuration, indicating the improved confinement of high energy electrons in this configuration. Note also that in the antiMirror case, the X-ray flux ends when the heating pulse is terminated. In the QHS configuration, the X-ray emission continues for more than 20 msec after the ECH is turned off.

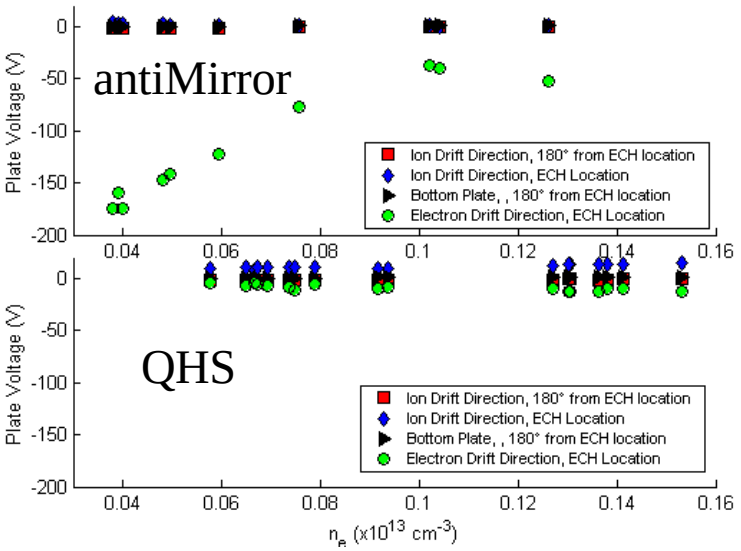

FIG. 4. Floating Potential on the four collector plates as a function of density in the QHS and antiMirror configurations.

As a direct measure of particle confinement, a series of collector plates has been placed at the plasma edge. Two of these plates are at the toroidal location of the ECH antenna, one in the electron drift direction, and one in the ion drift direction. A second pair of plates was positioned 180° toroidally displaced from the ECH location, but in otherwise identical positions. The plates were allowed to float with respect to the vessel and their potential was monitored. Fig. 4 shows the results of density scans in the QHS and antiMirror configurations. In the QHS configuration, the potential on all four plates is uniformly small. In the antiMirror configuration, the plate in the electron drift direction at the ECH location goes to a very negative potential, especially at low densities, while the three other plates stay at small constant potentials. This large reduction in the floating potential is consistent with deeply trapped electrons being heated in the ECH and then leaving the confinement volume on direct loss orbits.

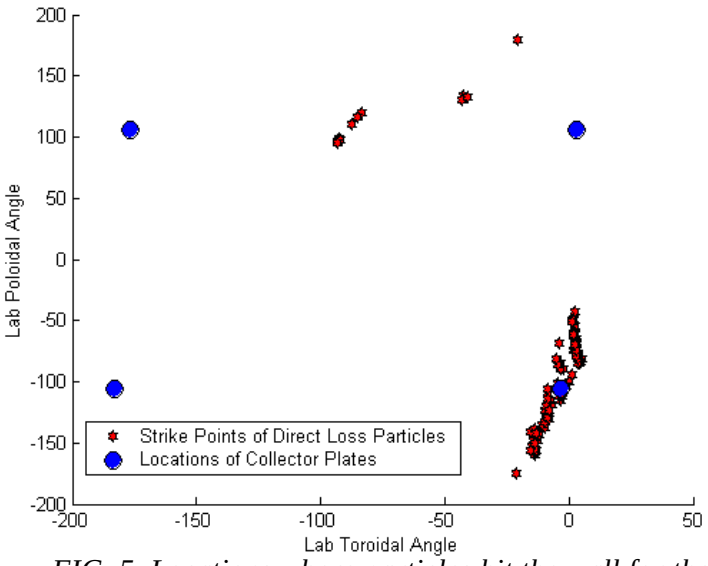

FIG. 5. Locations where particles hit the wall for the antiMirror case and locations of collector plates.

To test this hypothesis, we have used a guiding center code to launch 20 keV electrons at different locations and pitch angles

and computed their orbits until they intersected the vessel walls. Fig. 5 shows the locations where the particles strike the vessel in the antiMirror configuration; the coordinate system consists of the lab toroidal and poloidal angles. The locations of the collector plates are also shown. The particles on direct loss orbits strike the wall in bunches. The single plate whose location overlaps with the bunches is the plate with the large negative floating potential, supporting the conclusion that the direct loss mechanism is responsible for this plate's very negative potential. A similar calculation for deeply trapped particles in the QHS configuration shows that only a few particles launched at the very edge of the plasma strike the wall.

4. Flow Damping Rates.

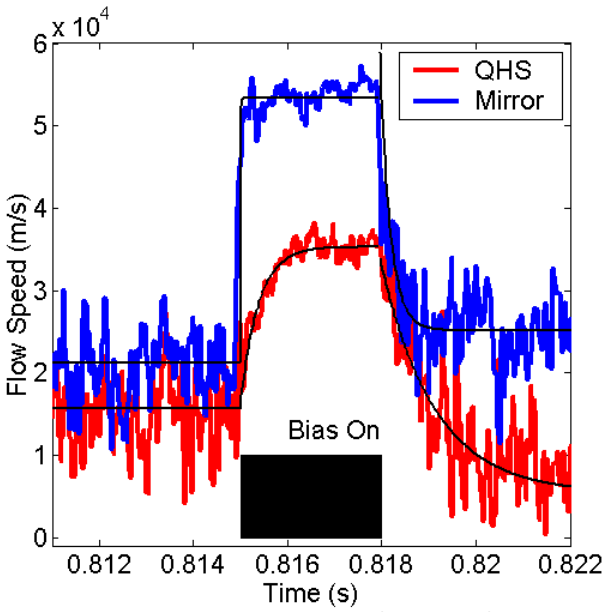

FIG. 6. Spin-up and decay of plasma flows in the QHS and Mirror Configurations.

We have designed a bias electrode/Mach probe system to measure the damping rate of ion flows in different configurations in HSX. The biasing electrode consists of a molybdenum electrode connected to a 600 V power supply capable of drawing up to 300A of current; electron saturation current to the electrode typically limits the collection to ≈20A. The power supply can be switched on and off in ≈20μs so that the spin-up or decay of the flow can be observed. To measure the flow with good temporal and spatial evolution, a 6 tipped Mach probe [4] has been implemented. The interpretation of the six ion saturation current measurements is done using the unmagnetized model of Hutchinson [5]. Finally, to estimate the charge exchange damping contribution to the total damping rate, an array of 16 H_α detectors has been constructed. Nine chords lie in a single vertical plane, and seven more detectors monitor the toroidal variation of the light. All detectors have been absolutely calibrated, enabling the collisional radiative modelling of Johnson and Hinnov [6] to estimate the neutral density from the H_α light and measured electron density profile [7].

Fig. 6 shows the flow speed for similar QHS and Mirror discharges with line average density of 1×10^{12} cm^{-3}. The stored energy in these two configurations at this density is comparable at around 20J. The timing of the electrode pulse is indicated at the bottom of the plot. The QHS shot is biased to 275 V and draws 5.7 A of electrode current and the Mirror shot is biased to 425V and draws 10.4A. The Mach probe is placed at a normalized radius (r/a) of about 0.8 in each case. As a measure of the damping rates, we fit an exponential to the rise of the flow speed. For the QHS configuration, the rise time is about .4 msec, while it is .1 msec for the Mirror configuration, indicating the lower damping rate in the QHS configuration.

We have made estimates of the damping rates using the model of Coronado and Talmadge [8]. In this model, the ion and electron continuity and momentum equations are solved under the assumption of no heat flux. Parallel viscosity in the limit of low rotation speed for either the plateau or Pfirsch-Schlueter regime and charge exchange damping are

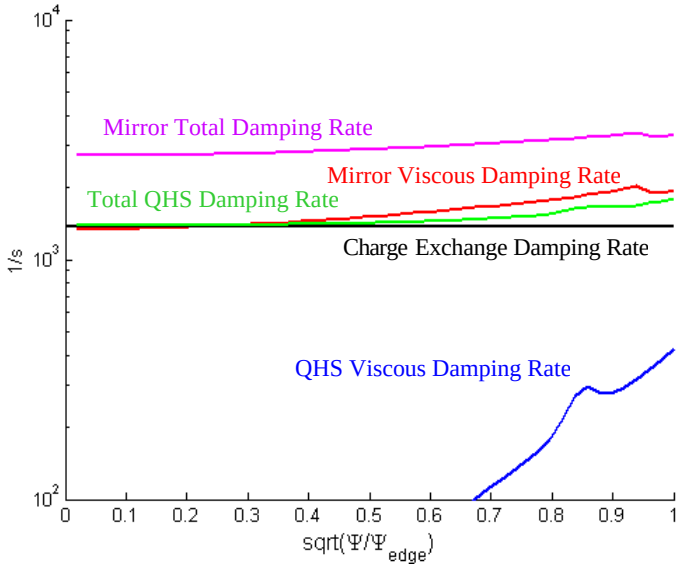

FIG. 7. Parallel viscous damping rates , the charge exchange damping rate, and the total damping rates, in the QHS and Mirror configuration.

both included as flow damping mechanisms. The model yields two expressions for the damping rate, corresponding to two directions on a flux surface, as well as the radial conductivity and the flow direction. The calculation is done in Hamada coordinates, and the basis vectors for a large aspect ratio tokamak are used [9]. We use a parabolic density profile matching the line integrated density and a flat ion temperature profile of 35 eV based on measurement of the impurity ion temperature using Doppler spectroscopy. This ion temperature puts the ions well into the plateau regime. Fig. 7 shows the damping rates due to parallel viscosity in the two configurations, as well as the damping rate due to charge exchange and the total damping rates. The Mirror configuration has a large parallel viscous damping rate across the entire minor radius which is of approximately the same magnitude as the charge exchange damping rate. The QHS configuration has a viscous damping rate which increases toward the plasma edge where small symmetry breaking terms in the magnetic field spectrum become larger. The total damping times at the plasma edge are approximately 0.6 msec in the QHS configuration and 0.3 msec in the mirror configuration. These numbers are in rough agreement with the damping times measured above.

5. Conclusions

The first results from the HSX stellarator confirm the expected advantages of quasisymmetric stellarators over more conventional stellarators. Experiments have shown that when the quasisymmetry is removed, the breakdown times are longer, the stored energy and hard X-ray fluxes are lower, and the viscous damping rates are higher.

References

[1] ANDERSON, F.S.B., ALMAGRI, A.F., ANDERSON, D.T., MATHEWS, P.G., TALMADGE, J.N., SHOHET, J.L., Fusion Technology 27, 273 (1995)
[2] TALMADGE, J.N., et. al., Phys. Plasmas **8** ,5165 (2001).
[3] CARTER, M.D., BATCHELOR, D.B., ENGLAND, A.C., Nuclear Fusion **27**, 985 (1987).
[4] PETERSON, B.J., TALMADGE, J.N., ANDERSON, D.T., ANDERSON, F.S.B., SHOHET, J.L., Rev. Sci. Instrum. **65**, 2599 (1994)
[5] HUTCHINSON, I.H., Plasma Phys. Control. Fusion **44**, 1953 (2002).
[6] JOHNSON, L.C., HINNOV, E., J. Quant. Spectrosc. Radiat. Transfer **13**, 133 (1973)
[7] DENG, C. el. al., to be published in Rev. Sci. Instrum.
[8] CORONADO, M., TALMADGE, J.N., Phys. Fluids B **5**, 1200 (1993).
[9] CORONADO, M., GALINDO TREJO , J., Phys. Fluids B **2**, 530 (1990)